

CY Cergy Paris Université
Laboratoire de physique des Lasers
Université Sorbonne Paris Nord

M2 Internship Report

**Construction of a high resolution imaging
system for a cold atoms experiment**

Author : Farid MADANI

Supervised by : Martin Robert-de-Saint-Vincent and Bruno Laburthe-Tolra

March 8th 2021 - June 23rd 2021

Table des matières

Introduction	1
1 Presentation of the imaging system	3
1.1 The imaging device	3
1.2 Constraints on the design	5
2 Opto-mechanics	6
2.1 The cage	6
2.2 Adjustment Mechanical components	9
2.3 Flip mirror	12
3 Optics	13
3.1 $f_0=100$ Lens	13
3.2 $f_1=300$ Lens	15
4 characterization of the imaging system	16
4.1 Protocol of characterization	16
4.2 Characterization	17
4.3 Vibrations	20
5 Protocol of installation on the experiment	22

Introduction

As a part of the Master's program at *CY Cergy Paris Université*, I did an internship in the *Laboratoire de physique des Lasers at Université Sorbonne Paris Nord*. I spent this period within the *Gaz Quantiques Magnétiques (GQM)* group, under the supervision of Martin Robert-De-Saint-Vincent and Bruno Laburthe-Tolra. I worked on the construction of a high resolution imaging system in the Strontium experiment.

The *GQM* group is working on two ultracold atoms experiments : The Chromium experiment, and the Strontium experiment in which I did my Internship. In this experiment, atoms of Strontium are cooled to very low temperatures, on the order of some nano-kalvins, in the purpose of studying dynamics of entanglement and magnetic order between atoms trapped in optical lattices. The isotope used in this experiment is the Strontium 87 (^{87}Sr), which is a fermion of a large spin of $F = \frac{9}{2}$, so it can go up to 10 different states. Strontium 87 presents also some interesting properties of interactions which consist in that interactions between two atoms don't depend on the spin projections, because the spin of ^{87}Sr is of purely nuclear nature. So the only magnetic interaction arises effectively from the Pauli exclusion principle.

Since the beginning of 2019 the group has succeed to get a degenerate gas of fermions. The present work of the group consists on preparing 2D optical lattices ; these lattices are made by the interference of two counter-propagating green laser beams of a wavelength of 532nm, creating a spatially periodic polarization pattern, which will be "cut" by an infrared 1064nm laser beam which creates a vertical potential, to get at the end many horizontal 2D lattices spaced by the same distance. The next step will be to load atoms in the lattice, they will be trapped at the minimas of the resulting periodic potentials (because of theses lattices being red-detuned lattices) to finally get an arrangement which resembles a crystal lattice.

The work that was assigned to me during this internship is to construct a high resolution imaging system that will be installed vertically on the experiment, on the top of the window of the vacuum, so we can have a top view on the optical lattices. The imaging system actually may serve two purposes : actual imaging of the atoms, and focusing of a targeting beam on them. Below I introduce briefly both. :

- The first use which is the imaging of the atoms ; can be done by the two techniques said : absorption imaging, and fluorescence imaging. Its purpose is the measurement of the density of the atom cloud or the distribution of atoms on the lattice and also the momentum distribution of the atoms.

In the case of the technique of absorption imaging ; the measurement of the density or the distribution of atoms in the lattice, can be done by sending on the atom cloud a collimated laser beam which is resonant with an absorption line of the atoms ; in our case we use a 461nm laser beam which is resonant with the transition $^1S_0 \leftrightarrow ^1P_1$ of the ^{87}Sr ; and the atoms will absorb a part of the beam. Taking the intensity of the beam before and after crossing the atoms, we can find density thanks to the Beer-Lambert law.

For the measurement of the momentum distribution, we do a "time flight" by swit-

ching off all trapping potentials (magneto-optical trap, optical dipole trap, and/or optical lattice, depending on the stage), in this case the atoms are in a free fall and their position at time "t" depend only on their initial velocities. So we can determine the momentum distribution at any time "t" by making a "time flight" and taking an image.

- The second use of the system is important for the future work of the group. It consists in focusing a 532nm laser beam on atom. This approach uses a super-resolution technique, to address atoms with a spatial resolution even better than the optical resolution limit of the imaging system, in the purpose of detecting or modifying their spins. This will give the group the possibility to control the spin state of atoms at each site, and so, create different magnetic phases to study their dynamics.

During this report, I will be presenting the work that I did all along this internship. I will start by a presentation of the imaging system that I built and all its specifications. Secondly, I will move to explain the construction and the opto-mechanical part of the system, and then explain the method used to set up the lenses in the system. After that, I will present a characterization of the imaging system, which was made as a verification of the characteristics for which the system was optimized for. In this context of verification, a part is dedicated to our investigation of the source of vibrations that we noticed in the system during this work of characterization. The final part will consist on presenting the preparations and the protocol we prepared for the installation of the system on the experiment.

1 Presentation of the imaging system

1.1 The imaging device

The imaging system that I built during this internship is a homemade system designed and optimized by the group specifically for the needs of the experiment ^{87}Sr . The decision of constructing a new imaging system for the experiment was taken essentially because the one currently present on the experiment does not fully meet the requirements of the group although it is very important for some specific tasks. One of the main disadvantages of this imaging system is having its principal planes (image and object plane) being vertical. The 2D lattices being in the horizontal plane, this imaging system does not give the possibility of taking images of these lattices unlike the new imaging system which will be installed vertically above the window of the vacuum. This means that its principal planes will be horizontal. An other advantage of this new system is its high spatial resolution. Indeed, it has a numerical aperture of $\text{NA}=0.20$ [1], which is the double of the numerical aperture of the horizontal imaging system $\text{NA}=0.10$ [2]. Calculating the Rayleigh criterion for this numerical aperture, we get :

$$\frac{1.22\lambda f}{d} = \frac{1.22\lambda}{2\text{NA}} = 1.4\mu\text{m}$$

where :

λ : is the wavelength, here $\lambda=461\text{nm}$

d : is the diameter of the lens.

f : is the focal length of the lens.

NA : is the numerical aperture of the lens.

This Rayleigh criterion specifies the minimum separation between two light sources that may be resolved into distinct objects. Having a smaller Rayleigh criterion means having a smaller diffraction limit. This, will allow taking images of smaller objects and thus doing more precise measurements on the atoms.

An important motivation also is to include in this new system the option of light focusing. This system being orthogonal to the optical lattices, it will give the possibility to focus a beam on the atoms to detect or to manipulate their spins.

In Figure 1 we can see how the two functions of the imaging device work.

The blue 461nm beam is the imaging beam, it illuminates the atoms from the bottom with a collimated beam. The lens f_0 is the most important part of the system. Its first task is to collect the light scattered by atoms. This lens is critical, because it is the element with the highest numeral aperture, 0.2, and thus the most susceptible to optical aberrations. Such a numerical aperture is especially difficult with long-focal-length objectives such as here. The role of f_1 is to refocus the light collimated by the lens f_0 and in the same time do a x3 magnification ; which consists of creating an image of the atomic cloud, magnified by a factor of 3. The lenses f_2 and f_3 are optional, they allow to do an other x3 magnification before the image is taken by the CCD camera. These

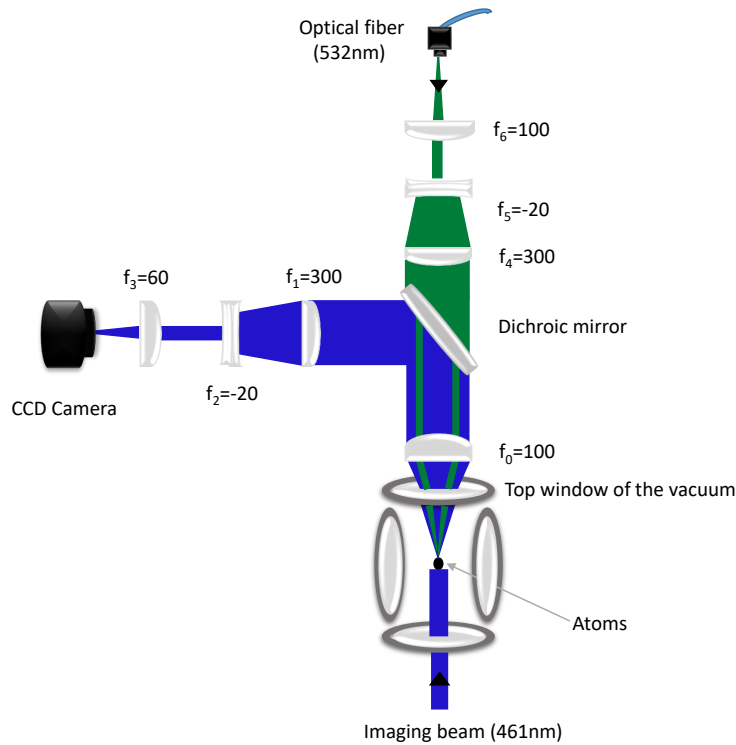


FIGURE 1 – Optical Scheme of the imaging system with the light focusing part. The blue part is the imaging part and the green one is the light focusing part. For the imaging beam, only the part scattered by the atoms is represented. The focal lengths are in mm.

magnifications are made because by enlarging the images of the objects we are not anymore constrained by pixelation limit of the camera. However, when the system will be in the experiment as a starting point, the magnification by f_2 and f_3 will not be installed because of the high quality of the camera. Indeed, the camera pixel size will be already well matched to the airy diameter of the imaging system point spread function, which seems an optimal compromise between resolution and signal to noise ratio considerations. So, this magnification will be made only in special cases

The Green 532nm beam is the focusing beam. It comes from an optical fiber and then is collimated by f_6 . The Lenses f_5 and f_4 work as a telescope which enlarges the beam to the size of f_4 . We come then to the second task of f_0 , which is to focus the beam on atoms.

Now that we know how these two functions of the system work, we can talk about the system to construct. When constructing the devise, I focused on the imaging part of the system since there is no need for the light focusing part for the moment.

In Figure 2 we can see the optical scheme of the imaging system with f_0 which collects the light scattered by atoms in absorption imaging method, or the photons emitted by the atoms in fluorescence imaging method. Then f_1 refocuses and in the same time magnifies x3 (for distance between the lenses equal to f_0+f_1) the collimated beam which then we

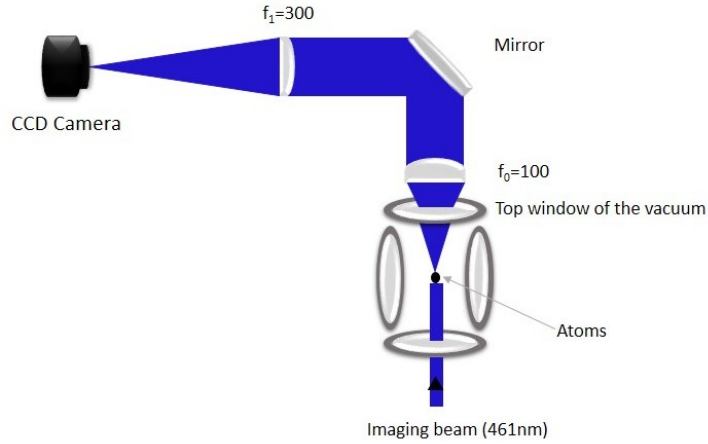


FIGURE 2 – Optical Scheme of the imaging system as built now - without the targeting beam (focusing beam) part. For the imaging, only the part of the beam that is scattered by atoms is represented. The focal lengths are in mm.

can detect in the camera.

1.2 Constraints on the design

One important constraint on the design of this Imaging system comes from the fact that its optical axis coincides with the vertical axis of the vacuum chamber. This coincides with one of the light beams of the Magneto-optical-trap(MOT) being in the vertical axis. To understand what the problem is, and which kind of constraint this beam imposes on the design of the system we need to talk about the MOT and the retro-reflection.

Retro-reflection :

The MOT is an apparatus which uses lasers and a spatially-varying magnetic field to create a trap where samples of cold atoms are trapped. A 3D MOT, like the one in ^{87}Sr experiment, is an arrangement of three pairs of mutually orthogonal and counter-propagating laser beams which intersect in a vacuum chamber containing the studied element, here the ^{87}Sr . Each of these pairs is used to slow the atoms in one of the directions of space. And so, in their intersection, they create a viscous region where a dumping force is exerted on the atoms. Here, the atoms will be slowed but this radiation pressure alone will not allow for their spatial confinement. To have an apparatus that can cool and confine atoms, we need to select the proper circular polarization for the beams and apply a quadrupole magnetic field.

The part that interests us here, and that gives a constraint on the design of the imaging system is the selection of the circular polarization of the two counter-propagating beams in the vertical axis. The most common way to set these pairs of counter-propagating beams with the correct polarization is to use retro-reflection method.

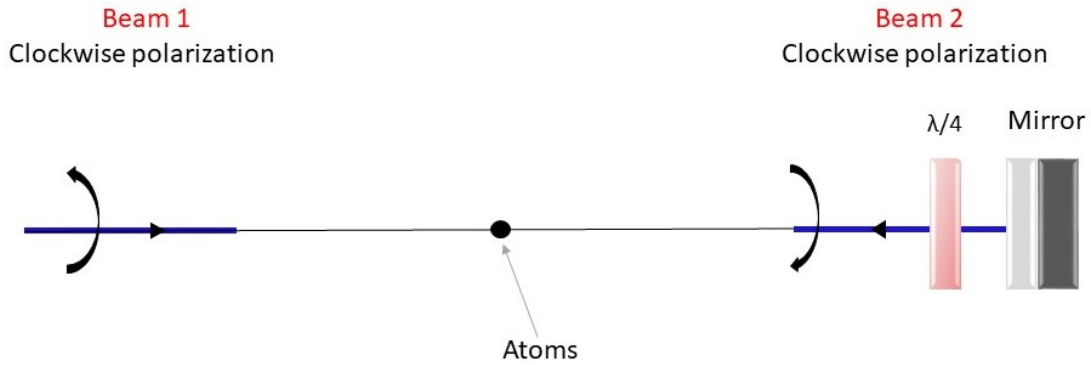


FIGURE 3 – Scheme of the components of the retro-reflection. The beam is coming from the left with a clockwise polarization. After passing and coming back through the quarter-wave plate, the beam goes in the opposite direction and the polarization remains clockwise.

Retro-reflection consists in reflecting a beam in a mirror and keeping the same polarization. The trick to keep the same polarization is to use a quarter-wave plate. So having, for the coming beam a clockwise circular polarization, it takes the opposite direction of propagation when being reflected by the mirror and gets the opposite angular momentum when passing two times through the quarter-wave plate. This defines a clockwise polarization for the retro-reflected beam.

The constraint on the design of the imaging device comes from having this retro-reflection setup in the vertical axis. Actually we can not avoid the MOT beam passing through the imaging lens f_0 , which is as close as possible from the top window of the vacuum chamber. The solution to this problem is to use a flip mirror with a voltage-controlled motor, so we can deviate the two beams of the MOT that will need to be retro-reflected (Blue 461nm for the transition $^1S_0 \leftrightarrow ^1P_1$ and red 689nm for the transition $^1S_0 \leftrightarrow ^3P_1$) to another axis, where we will install the quarter-wave plate and the mirror. An other constraint is, since the beam of the MOT will pass through the f_0 lens, it will be focused, so we need to ensure that the retro-reflected beam will be collimated. For this, we will need to add a $f=100\text{mm}$ lens to the retro-reflection components, to make the $f_0=100\text{mm}$ lens collimate the retro-reflected beam.

2 Opto-mechanics

2.1 The cage

The group opted to do this imaging system as a caged system. Caged systems, when being without big mechanical constraints on the optics, have the advantage to be rigid and to maintain the stability of the system. And especially in the case of the experience ^{87}Sr , the imaging system will need to be suspended above the window of the vacuum

chamber, so there is not many possibilities to install the optics and to ensure their stability.

We can see in FIGURE 4 how the cage will be maintained on the top of the vacuum chamber

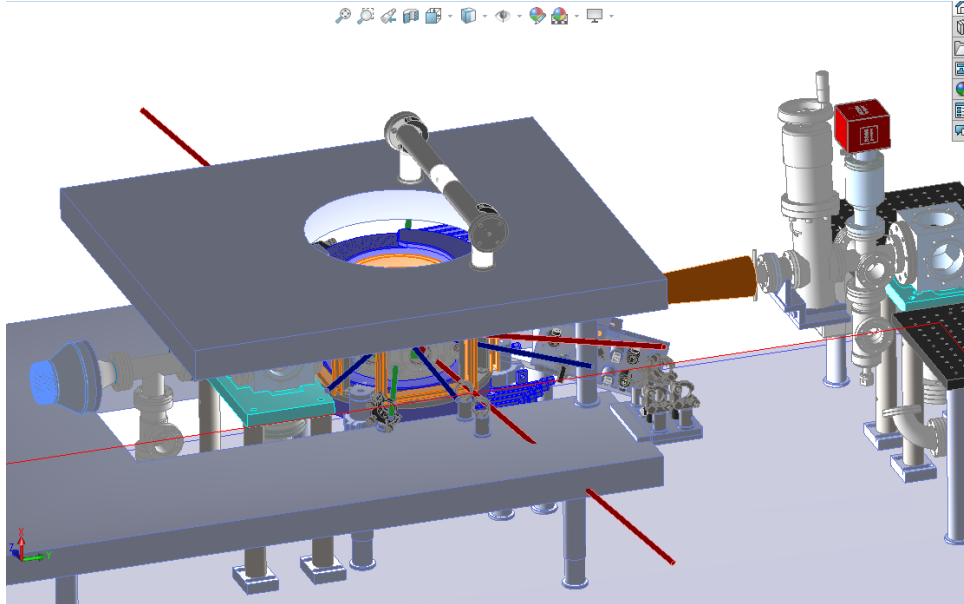


FIGURE 4 – The imaging device will be supported by an optical table with a hole on the top of the vacuum chamber. It will be maintained by an horizontal rod which is fixed on the optical table by two vertical rods, in a way to have the imaging device centered on the hole. And thus, centered on the vacuum chamber

This caged system will allow to have more possibilities of adjustments of the distances and angles between the imaging system and the vacuum chamber (Atoms).

In the scheme in FIGURE 5 we can see the opto-mechanics used for building the system. The width of the cage is 60mm, which gives a diameter of opening of 50mm.

- The components (1) and (2) construct a small cage of 20mm height between the two components, which corresponds to the thickness of the Lens $f_0=100\text{mm}$ (FIGURE 2). this lens being maintained only by a screw in component (1), we can make the top borders of the lens in contact with the component (2) to ensure its stability.
- The component (4) is constituted by two square plates fixed to each others by springs in 3 corners, in the fourth the corner they are only in contact by a screw. Component (4) is attached to the "small cage" constituted by (1) and (2) by the component (3) which is a coupler with external threads. All this will allow the possibility to adjust the angle of the lens $f_0=100\text{mm}$ using the screw of the fourth corner of (4), in a way to be orthogonal to the axis of the cage.
- The component (5) is for the rigidity of the cage, since the vertical part is long.
- Two irises were installed in the vertical and the horizontal part of the system, to give as later the possibility to center a beam on the axis of the cage, in order to

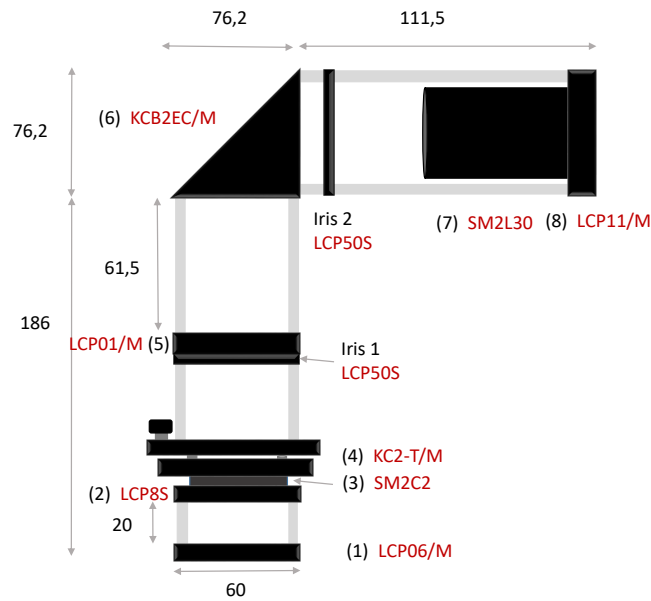


FIGURE 5 – Scheme in a profile view of the opto-mechanics of the imaging system. Lengths are in mm. In red the references of the opto-mechanics at Thorlabs.

set in place the optics.

- the distance between the Iris 1 and the mirror mount was chosen in a way to give enough space for the flip mirror.
- The component (6) is right-angle kinematic elliptical mirror mount. This mirror mount gives the possibility to adjust the angle and the plan of the mirror, which is important for centering light beams on the axis of the cage.
- the component (8) is a thick cage plate with internal threads that will allow to place the $f_0=300\text{mm}$ (FIGURE 2). Component (7) in a black lens tube attached to (8) which has as use to protect the light in the cage from light noise coming from outside the cage.

The components were assembled between them by cage assembly rods from **Thorlabs**.

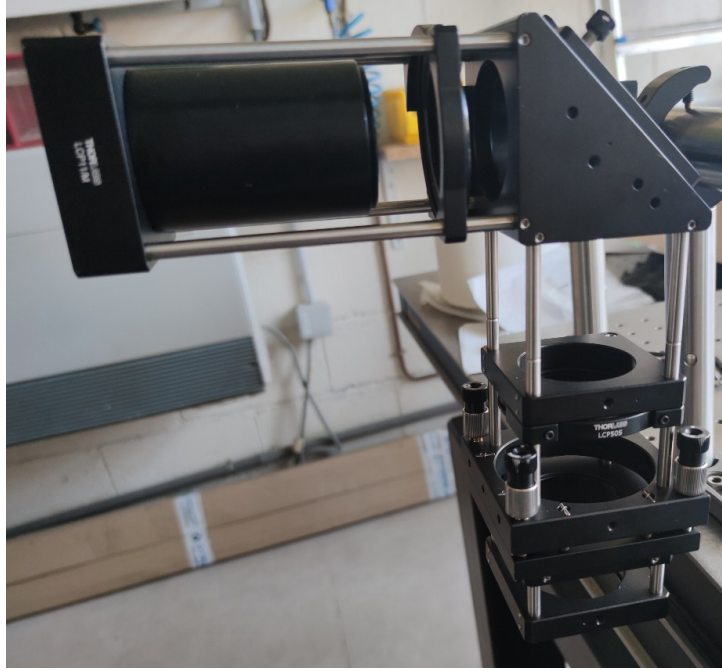


FIGURE 6 – Picture of the constructed cage of the imaging device before installing the lenses.

2.2 Adjustment Mechanical components

To ensure the possibility of doing relatively precise adjustments on distances and angles between the imaging system and the vacuum chamber, translations in the 3 space axis. and rotations on 2 axis were designed on the imaging system.

For the translation we used **Newport** XYZ linear stage (MODEL : M-460PD-XYZ), which is an ensemble of assembly of 3 translations in the 3 directions of space, the translation along **Z** being assembled with the translations along **X** and **Y** with a right angle component in which the translations are screwed.



FIGURE 7 – Newport XYZ translations (MODEL : M-460PD-XYZ)

These translations have **12,7 mm** maximum stage travel, and a integral locking mechanism to ensure the stability of the position. They also have a peg joining system for

flexible modulatory, this gives the possibility to put the 2 rotations on the system.

For the rotations, we initially opted for using the **Newport** rotation base (MODEL : M-460P-RA2). But after testing this rotation we realized that its locking mechanism was not strong enough to support the torque made by the weight of the system and the length of the horizontal and vertical parts of the system.



FIGURE 8 – Newport rotation base (MODEL : M-460P-RA2). We see in the center the hole of the axis of rotation, with two tightening screws. The diameter of the hole is too small, so it does not hold the torque.

To solve this problem of rotation we had to think for a homemade solution for each of the two rotations.

For one of the two, the solution was not very complicated to find. Since the system, when being installed in the experiment, one of its translation will be screwed to a 1.5 inches horizontal rod by the same way as in FIGURE 9.

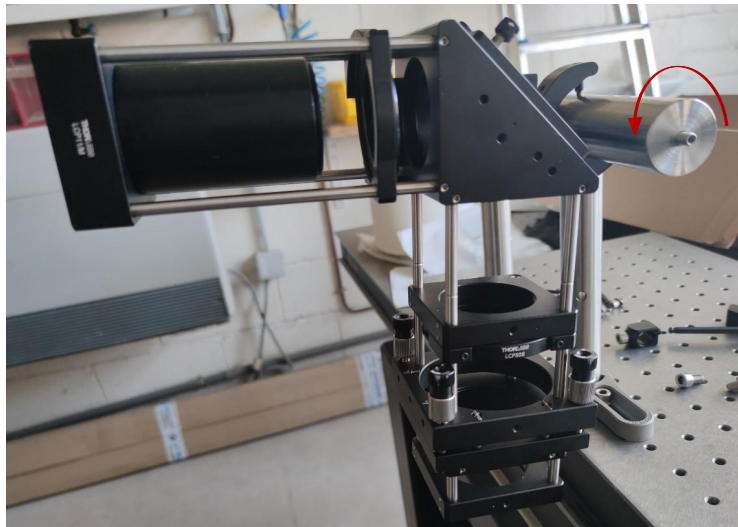


FIGURE 9 – Solution for the first rotation. Note the red arrow illustrating the rotation degree of freedom.

The idea is to take advantage of the fact that this rod is along one of the axis that we want to rotate the system around. So, to rotate the system around this axis, we just

need to rotate the horizontal rod, which has a good locking mechanism that can support the torque made by the system.

For the second rotation, for which the axis is in the same plane as the axis of the first rotation and is orthogonal to it, we were inspired by the locking mechanism that was used for the horizontal rod, to modify the **Newport** rotation base. The modification that we performed on the rotation base was firstly to enlarge the axis of rotation by enlarging the whole on the center of the rotation base to 1.5 inches, then we screwed on it the locking mechanism that was used for the horizontal rod, we can see this in FIGURE 10. Attaching a small 1.5 inch rod to one of the translations of the system, we can put this rod on the rotation and well lock it. This homemade rotation supports the torque made by the system.

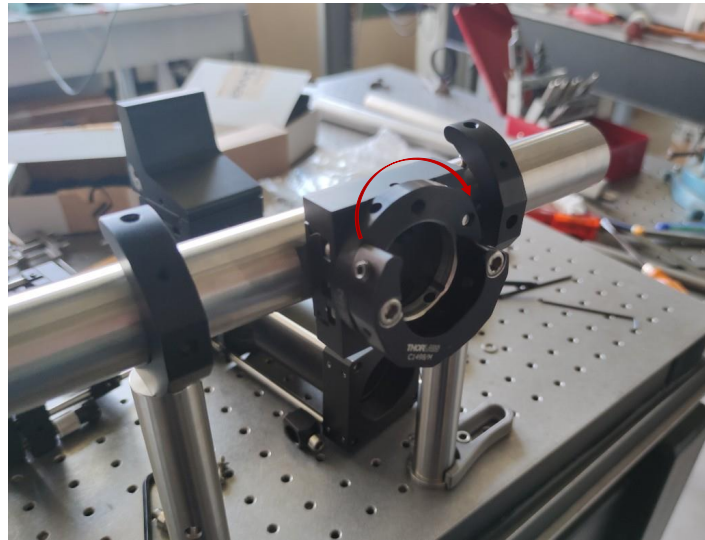


FIGURE 10 – Solution for the second rotation. Note the red arrow illustrating the rotation degree of freedom.



FIGURE 11 – Top view of the imaging system locked by the two rotations

In FIGURE 10 The surface of the horizontal rod to which the outest translation is fixed, was flatten to have a full contact between the two surfaces, and to avoid instabilities when tightening the screws.

We can see in FIGURE 11 the system locked with the two rotations. We see also the way the system is fixed in the second rotation.

2.3 Flip mirror

Like explained before, there is a constraint in the construction of the imaging system which is due to the retro-reflection of the beams of the MOT. The solution to this constraint was to install a flip mirror which can cut the axis of the imaging system and deviate the beams of the MOT to the direction where we will install the components of the retro-reflection. This forced us to remove one of the rods of the cage so that the flip mirror can enter the cage.

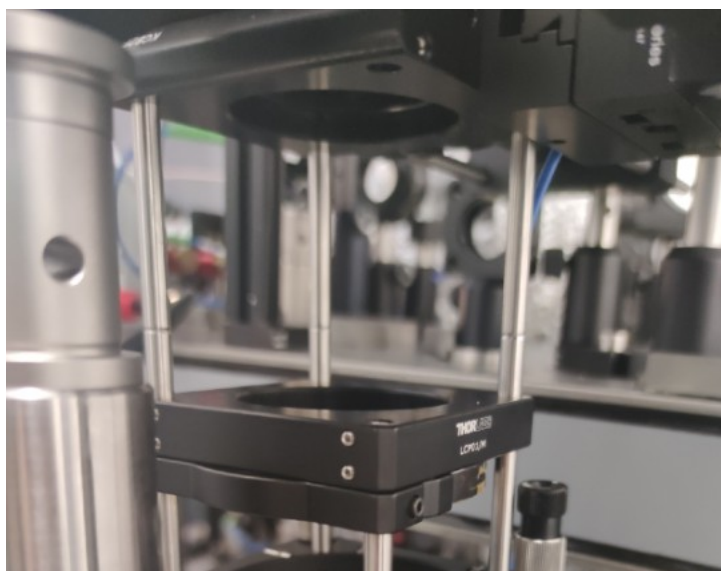


FIGURE 12 – A rod is removed to the cage where the flip mirror will enter the cage

For this flip mirror we will use a motorized filter flip mount with a 1 inch optic holder from **Thorlabs** (MODEL :MFF101/M) in FIGURE 11

The Motor of this component can be used by 3 different methods. It can be used manually or by using a code on a computer, but we are not interested in these two methods. We are interested in the last method which consists on controlling the component by its external SMA connectors. The flipper position rotates 90° clockwise or counterclockwise when it is toggled. To toggle the mirror mount attached to the motor, we will use an edge signal, which means that a rise of the control voltage to 5V causes the flipper to rotate. More clearly, at each time the motor receives 5V, the flipper switches from a position to an other of the two possible positions. The unit has magnetic limit switches at both positions to identify at which position the flipper is in.

We chose this method of using this component because the ^{87}Sr experiment is working



FIGURE 13 – Motorized filter flip mount from **Thorlabs** (MODEL :MFF101/M)

with a software that controls electrical generators. So we can simply connect the SMA connectors to a tension generator, then we can control the flip mirror directly by the software of the experiment by controlling the voltage.

3 Optics

After finishing the construction of the cage of the imaging system I moved to place the optics in this system. To correctly place the optics we have to ensure the correct distance between optics, center the optics such that the optical axis coincides with the axis of the cage and make the surface of the the lenses orthogonal to the axis of the cage.

3.1 $f_0=100$ Lens

The $f_0=100$ mm lens is used as a focusing objective. It is a multi-element lens, composed by 3 lenses. It was especially made for the needs of the ^{87}Sr experiment, so that it has a large numerical aperture of $\text{NA}=0.20$ to have a high resolution imaging, and it also compensates the aberrations due to the glass of the window of the vacuum chamber. The disadvantage of this lens is that, because of being a thick lens with a large numerical aperture, this lens is very sensible to aberrations. So, it needs precise installation in the cage.

To install the $f_0=100$ mm lens. I placed the system in almost the same conditions as it will be in the experiment, this by fixing its outest translation to an horizontal 1.5 inch rod as in FIGURE 11 but this time in the optical table of the experiment.

After this, the first task was to collimate a blue 461 nm beam coming from an optic fiber. Then, to have a control on the horizontal and vertical angles of the beam and on its plan I used two mirrors as in FIGURE 14.

After having this in place, I started by centering the beam on the axis of the cage by closing the two irises in the horizontal and in the vertical part of the cage to a minimum

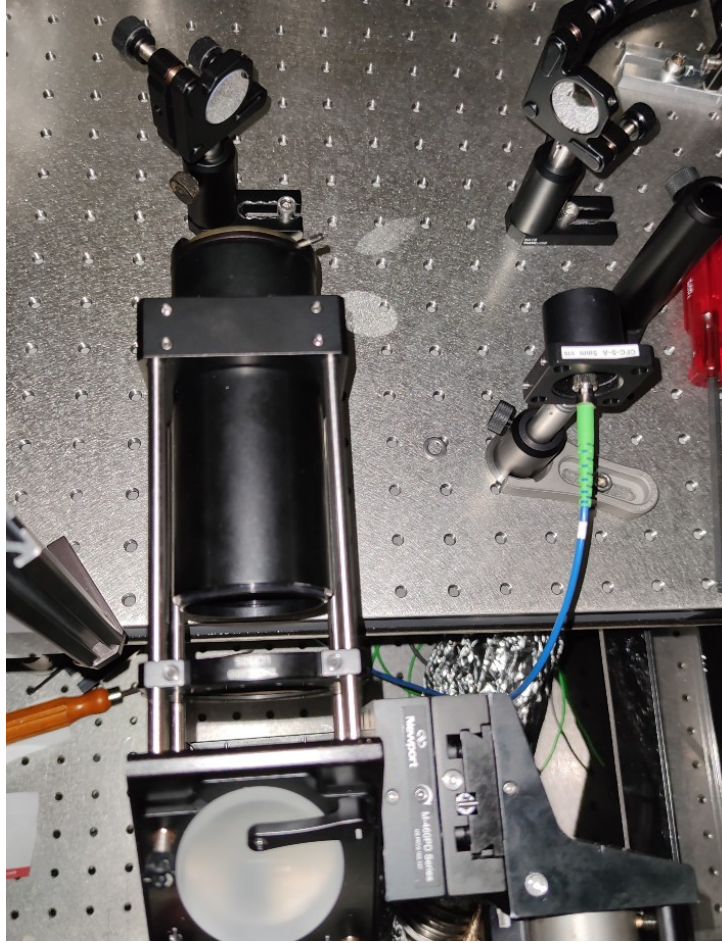


FIGURE 14 – Picture of the installation while centering the $f_0=100\text{mm}$ lens

opening. I also placed an iris in the entrance of the horizontal part of the cage by outside, to simplify the alignment. And then, I worked on adjusting the angle and the plan of the beam using the two mirrors to pass the beam through the centers of all the irises.

The beam centered in the axis of the cage, I placed the the $f_0=100$ lens on the imaging system, and I had to ensure that it is orthogonal to the beam that I centered on the cage. To do this, I had two degrees of freedom. The first one was the angle of the lens itself, which I could adjust using the component (4) in FIGURE 5, this component gives the possibility to change the horizontal and vertical angle of the lens. The second degree of freedom was to change the angle and the plan of the mirror of the cage.

What essentially help us to fix the orthogonality of the lens in the cage is the retro-reflections on the lens. The lenses are in general treated anti-reflections but it is never perfect. So we take profit from this fact, and to make the lens orthogonal to the axis of the cage we need to superpose the coming beam on the lens and the retro-reflections of the surface of the lens.

The way I proceeded to place the lens was by using the mirror is a guide. More clearly, I translated back the mirror until the the end of the translating screws and then, I started translating it in the other way by small steps. At each step, I tried to adjust the angles

of the mirror in the same plane, and the angles of the lens. Going on with the translation of the plane of the mirror step by step, I succeeded to find the plane of the mirror where, with adjusting its angles and the angles of the $f_0=100\text{mm}$ lens, I could superpose the coming beam with the retro-reflections on the lens.

3.2 $f_1=300$ Lens

The $f_1=300$ lens used in this system is a cemented achromatic doublet. It is reasonably corrected from spherical aberrations.

Comparing to the $f_0=100\text{mm}$ lens, $f_1=300\text{mm}$ is less sensible for aberrations, because it is thinner and it is used with lower numerical aperture. Because of being less sensible, its installation was easier than the installation of the $f_0=100\text{mm}$ lens.

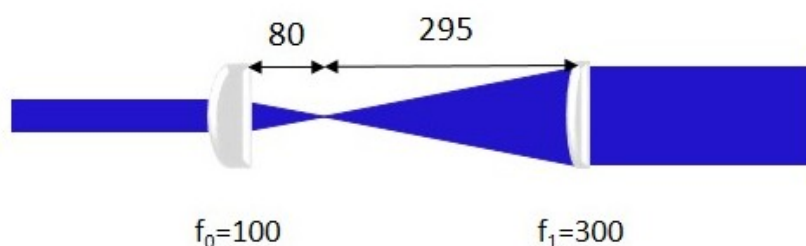


FIGURE 15 – The imaging system working as a telescope. The distance measured between the two lenses is $375\text{mm} \pm 5\text{mm}$, the $f_1=300\text{mm}$ lens being much thinner, with specified back focal length of 295 mm . Roughly speaking, it means that the $f_0=100\text{mm}$ lens has a back focal length of order of $80\text{ mm} \pm 5\text{ mm}$.

In FIGURE 15 we see that the system is working as a telescope. When sending a collimated beam from one side it comes out also collimated. So, to install the $f_1=300\text{mm}$ lens, I used a collimated beam coming for the right ($f_1=300\text{mm}$ lens side), and looking at a long distance to the beam after coming out from the system, I was changing the position of the $f_1=300\text{mm}$ lens until I got a collimated beam, and I fixed the lens on the cage.

For the orthogonality of the lens to the axis of the cage, I initially trusted the construction of the cage, because there was no apparent construction defects. After fixing the lens I verified the retro-reflection of the lens and they were correctly superposed on the coming beam.

An interesting remark is that the distance between the two lenses is not $f_0+f_1=400\text{mm}$, and that is because of the $f_0=100\text{mm}$ lens which is actually a high quality lens constituted by 3 lenses assembled together.

After installing the $f_1=300\text{mm}$ lens, I measured $375\text{mm} \pm 5\text{mm}$ distance between the two lenses. Taking the back focal length 295mm of the $f_1=300\text{mm}$ from the information sheet of the lens, we can deduce that the working distance of the $f_0=100\text{mm}$ lens is $80\text{mm} \pm 5\text{mm}$.

4 characterization of the imaging system

After finishing the construction of the imaging system, we decided that it will be interesting to characterize it. To do this I set the same protocol of characterization made in [1] by a former intern in the group.

4.1 Protocol of characterization

The characterization of this imaging system consists in setting a protocol by which we can define the limit of resolution of this system. To do this, the first method, that we can use, is to take small objects separated by a very small distance, and take an image of them using the imaging system. The smallest distance between the two objects which can be resolved by the imaging system is what will define the limit of resolution.

This method was envisaged in a former internship where an intern characterized a prototype of this imaging system [1]. But this method is not simple to set since the limit of resolution of this system is in order of $1.4\mu\text{m}$. No small object separated by this distance are available in the group.

The other method that was used in [1] and that I also used is taking profit of the light focusing part of the system. The idea is to use the imaging system to focus a beam, as in FIGURE 1, and then to take an image of the spot at the focus. The size of the Airy disk of this spot will give as a pessimistic estimate of the limit of resolution of the imaging system.

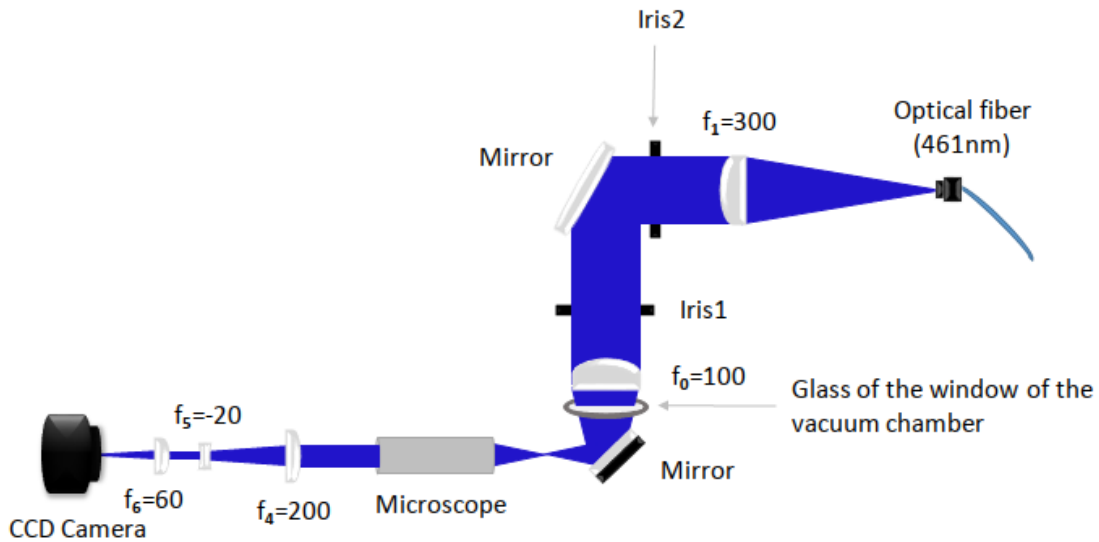


FIGURE 16 – New Protocol for the characterization of the imaging system, using directly the light coming from the optical fiber. Distances are in mm

In FIGURE 16, a blue 461nm divergent beam coming from the optical fiber is centered on the imaging system. It enters the imaging system from the $f_1=300\text{mm}$ lens. Then

the beam is focused by the $f_0=100\text{mm}$, and it passes then in a small version of the window of the vacuum chamber, made by the same glass. A high quality microscope of a numerical aperture of 0.25 of the mark Mitutoyo is used with a $f_4=200\text{mm}$ lens to do a x10 magnification. After that, a x3 magnification is made by using a $f_5=-20\text{mm}$ then a $f_6=60\text{mm}$ lenses. we finally get a x30 magnification, which is made to avoid getting limited by the limit of the pixelation of the camera, which has a pixel size of $7.4\mu\text{m}$. At the end, an Image of the spot in the focus is taken by a CCD camera.

4.2 Characterization

The characterization that we wanted to perform on this imaging system consists on determining its resolution limit. The procedure to do this, is to take the images taken by the protocol above and use Python to fit them by a function with a parameter related to the radius of the Airy disk.

Because of the limitation of the $f_3=-20$ lens that I had (which creates aberrations because of its small size), I changed the protocol that I used initially. In this initial protocol, the $f_3=-20$ lens was used to diverge the light collimated after the optical fiber. In the new one, in FIGURE 16, I used directly the divergent light coming from the optical fiber.

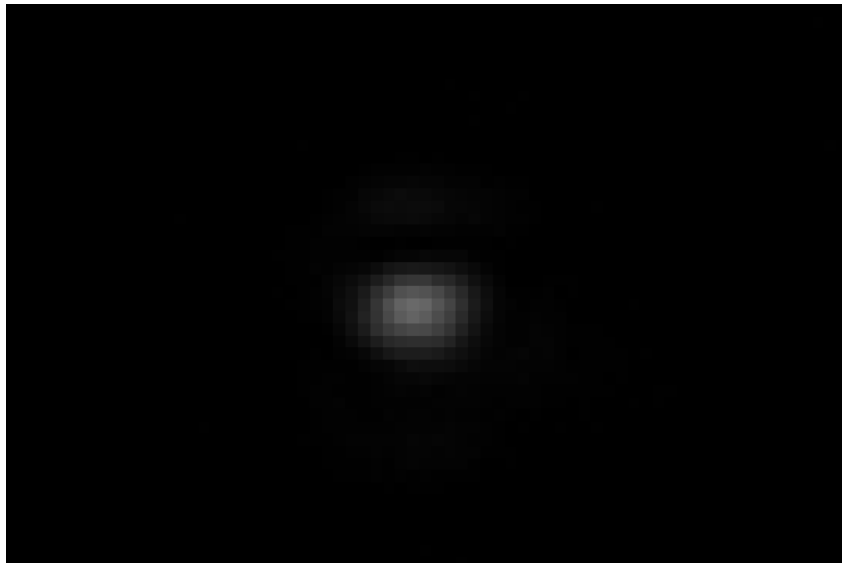


FIGURE 17 – Zoom on the image of the spot on the focus. We can see the the spot is not completely circular.

In FIGURE 17 we can see a zoom of an image of the spot. By translating the camera along the optical axis of the the Mitutoyo microscope and the $f_4=200\text{mm}$ lens, I found the focus of the $f_4=200\text{mm}$ lens and took this image. The spot that I got is not completely circular, this can come from the beam not being well centered on the optics of the protocol. I tried anyway to get the size of the spot, to have an idea about the resolution limit that the imaging system can attend. To do so, I did both a vertical and

an horizontal cross-section of the center of the spot, and fitted the points with an Airy function :

$$I(x) = A\left(\frac{2J_1(a(x - x_0))}{a(x - x_0)}\right)^2 \quad (1)$$

where J_1 is the first kind Bessel function.

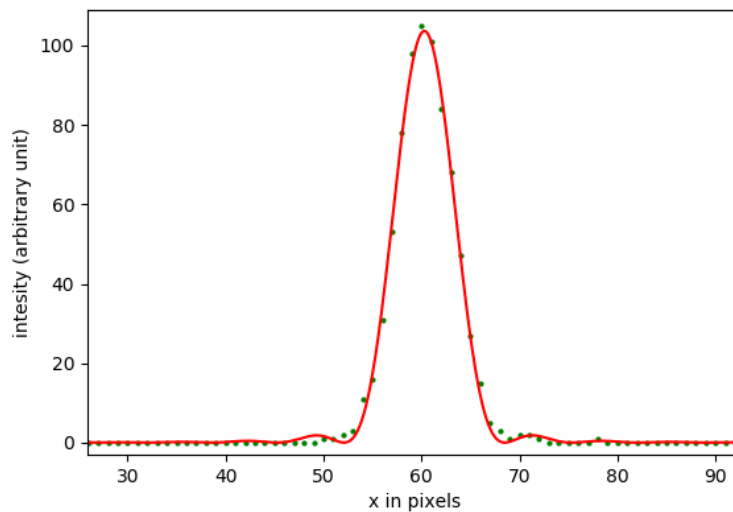


FIGURE 18 – Fit of the horizontal cross section of the center of the Airy disk in FIGURE 17. $a=0.47 \text{ px}$

The radius R of the Airy disk corresponds to the first "zero" of the Airy function, so :

$$I(x)=0 \iff \delta x = x - x_0 = \frac{3.83}{a}$$

$$\delta x = 8.15 \text{ px}$$

The size of the pixels of camera being $7.4 \mu\text{m}$; we get :

$$\delta x = 60.30 \mu\text{m}$$

Finally, we get the radius of the Airy disk by dividing δx by the x30 magnification, so :

$$R_h = 2.01 \mu\text{m}$$

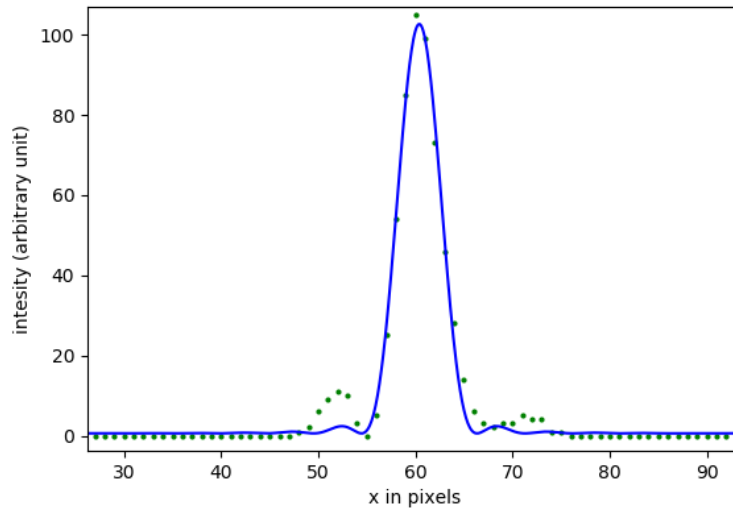


FIGURE 19 – Fit of the vertical cross section of the center of the Airy disk in FIGURE 17. $a=0.64 \text{ px}$

For the vertical cross section we get : $R_v=1.48 \mu\text{m}$

The Airy radius found for the vertical cross section is close to the theoretical Airy radius expected for this imaging system which is of order of $1.4\mu\text{m}$. But the Airy radius of the horizontal cross section is much bigger than $1.4\mu\text{m}$. To get better results on the spot, one should try to recenter the beam on the imaging system, then on the part of magnification. I think that the problem is more likely to be in centering the beam on the Mitutoyo microscope, because I noticed non-symmetrical rings on the beam coming from it, and which I couldn't see on the beam before the microscope.

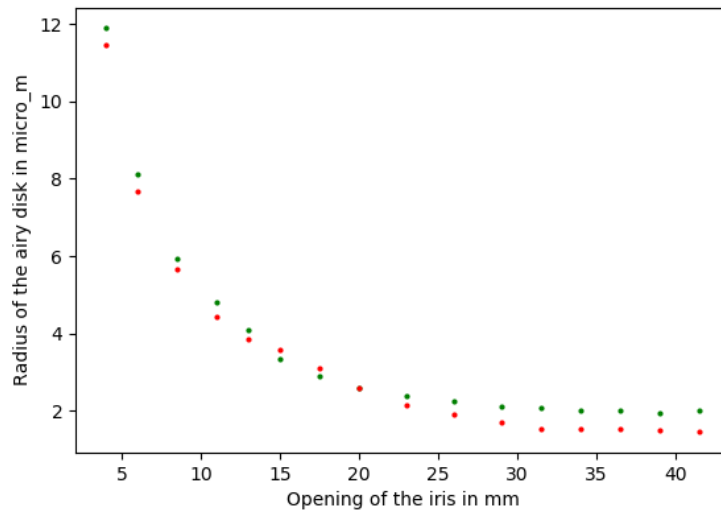


FIGURE 20 – Airy radius for different openings of iris 2, for the horizontal cross section (in green), for the vertical (in red).

A way to have an idea about the problem, and to compare the results to theory, was to measure the size of the Airy radius of each cross section, for different opening of the Iris 2 in the protocol in FIGURE 16. From theory, the radius of the airy disk should vary proportional to $\frac{1}{d}$. where "d" is the opening of the iris.

We can see the results in the FIGURE 20. We see that the two plots do not vary the same way, and the form of the plots does not give us much information. So the thing to do, is to try to realign the beam on the system carefully, and also use a more precise way to find the focus with the camera, by using a translation.

4.3 Vibrations

When doing the characterization of the system, we noticed on the camera important vibrations of the imaged spot. I tried then to investigate the source of these vibrations.

The first thing that I investigated was whether the vibrations were coming from vibrations of the camera and not of the spot. To do this, I tried to stiffen the rods that were supporting the camera and the to compare to the vibrations before and after changing the rods.

The camera was fixed to an horizontal 0.5 inch rod which was fixed on a vertical height adjustable 0.5 inch rod. I took 50 images of the spot the camera being supported by these two rod. Then, I replaced the two rods by two 1 inch rods and took also 50 images of the spot.

Using Python, I calculated the standard deviation for the positions in vertical axis of the images, for the central pixel(most illuminated pixel) of the image of the spot :

- $\sigma=0.76\text{px}$ for the camera supported by 0.5 inch rods.
- $\sigma=0.74\text{px}$ for the camera supported by 1 inch rods.

There is no significant difference between the two measures using the two sizes of rods, so we can conclude that the vibrations do not come from the camera.

After the camera, I investigated the vibrations of the Mitutoyo microscope. This time because of the sensibility and the difficulties to align the microscope, I did not change the rod supporting it but I tried to dampen the vibrations of the microscope by putting a weight on it. So, I put a weight on the microscope and took 40 images to compare to the standard deviation when there is nothing to dampen the vibrations :

- $\sigma=0.81\text{px}$ when there is no weight on the microscope.
- $\sigma=0.55\text{px}$ when there is a weight on the microscope.

There is a significant difference between the two standard deviations. So, a part of the vibrations comes from the Mitutoyo microscope.

Although there were a progress by damping the vibrations of the microscope, the image of the spot on the camera was still vibrating. The thing to investigate after that, was the imaging system itself. And that, by trying to fix it to the optical table without

putting too much constraints to not disalign the beam on the cage.

I had many possibilities to try to dampen the vibrations of the system :

- Fix the horizontal part of the cage to the upper optical table.
- Fix the vertical part of the cage to the bottom optical table.
- Fix the vertical part of the cage to the upper optical table.
- Fix both horizontal and vertical part.

I present in the following table the results of the measurements that provide interesting information for the damping of the vibrations.

These measurements are made with the vibrations of the microscope being damped.

	Only Horizontal part		Vertical part to the upper optical table + Horizontal part		Vertical part to the bottom optical table + Horizontal part	
	NO	YES	NO	YES	NO	YES
Standard deviation (px)	1.04	0.71	0.93	0.70	0.93	0.16

FIGURE 21 – Table of the standard deviations of the measurements on the position of the spot on the camera for different fixings of the imaging device.

In FIGURE 21 we see the standard deviations for the three different situations. For the two first situations ; fixing only the horizontal part of the imaging device and, fixing the vertical part of the imaging device to the upper optical table (with the horizontal part still fixed), there is a significant decrease of the standard deviation, but there is not much difference between the two cases.

For the last case, when fixing the vertical part of the imaging device to the bottom optical table (with the horizontal part still fixed), there is a large decrease of the standard deviation. which means a great suppression of vibrations. This is probably because of fixing the $f_0=100\text{mm}$ lens, which is has a big sensibility.

So from these results, the "ideal" when installing the system on the experiment is to fix its horizontal part to the upper optical table, and the vertical part to the bottom optical table. Practically this is difficult to do, because the bottom of the cage of the system is only 1mm away from the window of the vacuum chamber.

In the last days of the internship, one of the members of the group pointed out the possibility of the vibrations coming from the fan used to keep the heat of the oven away from the optical table. So I calculated the standard deviation of the measurements on

the position of the spot when the fan is on and when it is off. I got these results :

- $\sigma=0.60\text{px}$ when the fan is on.
- $\sigma=0.24\text{px}$ when the fan is off.

These measurements were done with the horizontal part fixed to the optical table.

We can see that most of the vibrations come from the fan. I tried to dampen the vibrations of the fan by putting pieces of Sorbothane between the fan and its fixation on the optical table, and by replacing its screws by plastic screws, but it did not change anything on the vibrations.

The things that are still to do to further optimize the vibration damping, is firstly to separate the fan from the optical table. This can be done by fixing the fan from the top to the frame which is on the top of the optical table. An other thing to do, is to use the damping rod instead of the rigid horizontal rod, to see if it dampens the vibrations.

Besides this investigation of vibrations, we should notice some differences between the installation here and in the the experiment. The main difference is that, the vertical rods that maintain the horizontal rod to which the system is fixed, have a length of about 400mm. But in the installation on the experiment, the vertical rods will have only 60mm. This can damp the vibrations.

5 Protocol of installation on the experiment

We prepared a protocol for the installation of the imaging system on the experiment in advance to avoid any surprises. This is especially because of the risk of hitting the window of the vacuum with the imaging system due to the very small distance between them, which is of the order of 1mm. An other reason also, is that for centering the imaging system we need to use the atoms as a target, so we need to know in advance the procedure to realize this

The imaging system will be installed on the experiment as it was installed for tests in FIGURE 11. An horizontal 1.5 inches rod will be fixed to the optical table by 1.5 vertical 1.5 inches rods. The imaging system will be maintained to this horizontal rod, by fixing its outest translation to the rod by 2 screws.

We see in FIGURE 22 a scheme of a front view of the imaging system installed on the optical table of the experiment. In the same figure, the flip mirror is also installed on the optical table, to which it will be fixed by 2 height adjustable 0.5 inch rods. The electrical wires that will be used to control the motor will be fixed along the horizontal rod.

After fixing the imaging system on the horizontal rod and the flip mirror on the optical table, the task will be to center the cage on the axis of the vacuum chamber, and then to make the axis of the cage orthogonal to the top window of the vacuum chamber. To do these two steps we need to use the atoms as a target in the center of the vacuum

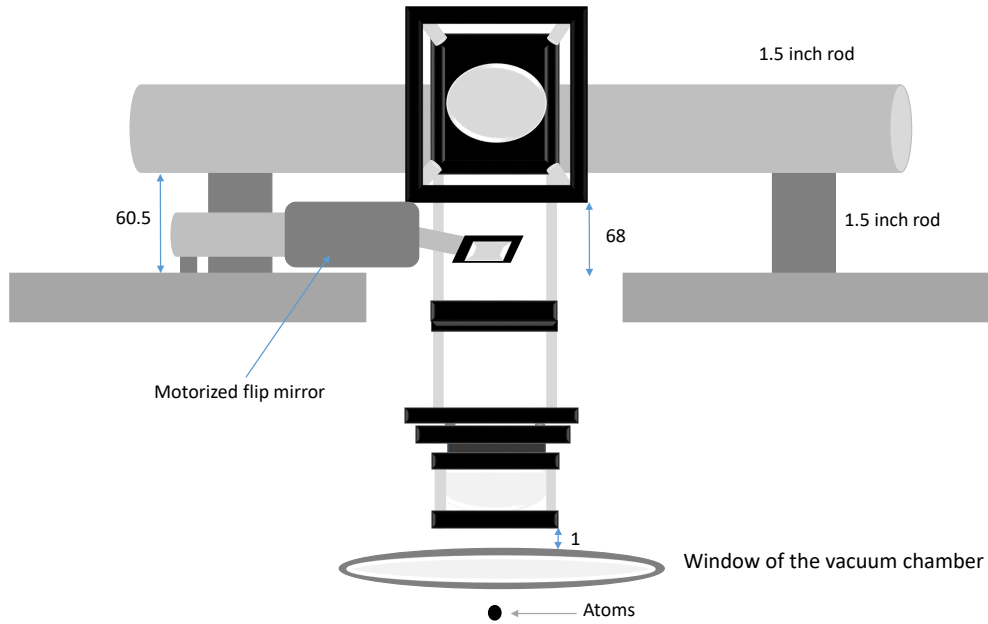


FIGURE 22 – Front view of the imaging system as it will be installed on the experiment.

chamber. So, we need to install the retro-reflection components, to be able to trap the atoms in the center of the vacuum chamber.

Retro-reflection The components of the retro-reflection as we can see in FIGURE 23 will be fixed sideways to a 1 inch rod below the horizontal part of the imaging system. The only constraint is on the $f_2=100\text{mm}$ lens, which needs to be at a distance of 180mm from the $f_0=100\text{mm}$ lens, according to the back focal length of f_0 which is 80mm as measured earlier. The $f_2=100\text{ mm}$ lens is used to recover the collimation of the magneto-optical trap beam.

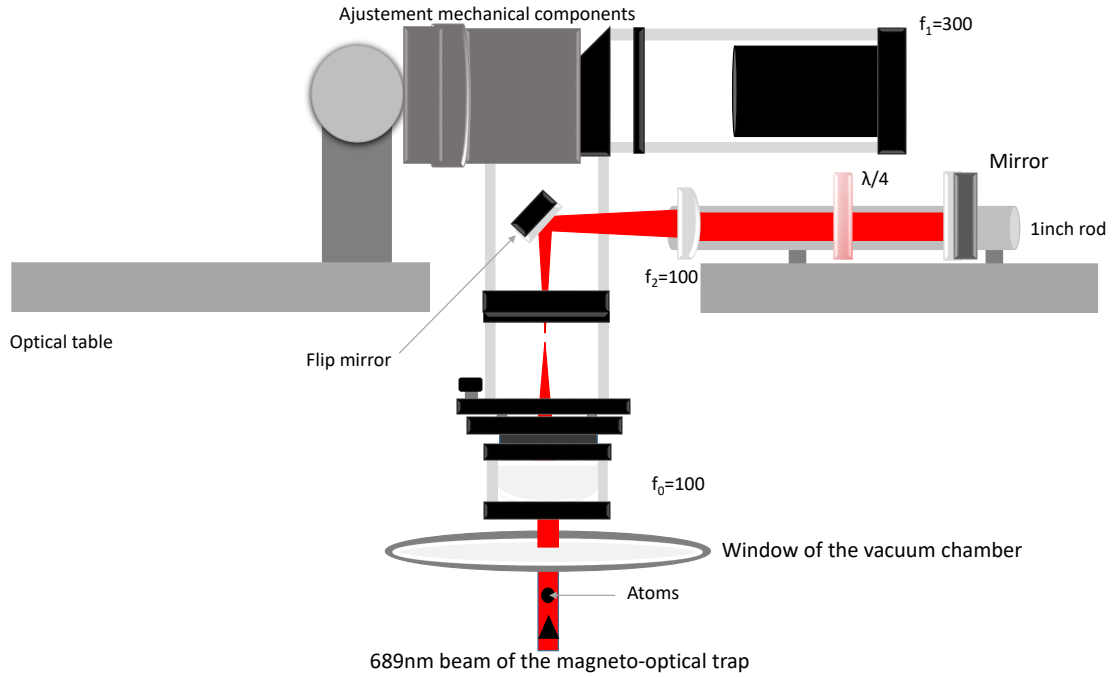


FIGURE 23 – Installation of the retro-reflection components after installing the imaging system. The represented red 689nm beam is the beam of the magneto-optical trap which is exploiting the transition $^1S_0 \leftrightarrow ^3P_1$. A blue 461nm beam which is exploiting the transition $^1S_0 \leftrightarrow ^1P_1$ will also be retro-reflected in the same way

Final adjustment After fixing the retro-reflection components, time will be for centering the imaging system. To do this we need to switch on the magneto-optical trap and trap the atoms on the center of the vacuum chamber. Then, we fix an optical fiber on the entrance of the horizontal part of the cage and target the atoms with the coming beam. Using the adjustment mechanical components we can translate and rotate the imaging system to have the beam pointing to the atoms and orthogonal to the top window of the vacuum chamber at the same time. We verify the orthogonality by superposing the beam with the retro-reflections coming from the window. When this is done, we can lock the translations and the rotations.

Conclusion

The first part of the internship, consisting in the opto-mechanical and optical construction of the imaging system was successfully done. I worked in this part on development of the design of the imaging system, especially on the mechanical components which will be used for adjustments during its installation. I was also able to detect sensibilities to vibrations in the system, and to propose protocols to minimize them. I focused on the last part of the internship on completing the characterization of the system, and on optimizing the attenuation of the vibrations.

These two tasks being not completely finished, I gave, at the end of each part, ideas about the remaining problems, and the things that are still to do.

Références

- [1] Romain Cazali, Internship report : "Optics and poly-chromatic high resolution of a cold atoms experiment"
- [2] Nicolas lecoeur, Internship report : " Absorption imaging system for a cold atoms experiment"
- [3] Metcalf J. "Laser cooling and trapping"
- [4] K. Kowalski, V.Cao Long, K.Dinh Xuan, M.Głódź, B.Nguyen Huy, J. Szonert "Magneto-optical Trap : Fundamentals and Realization" January 2010
- [5] Melles Griot "Fundamental Optics"
- [6] Cours de physique des lasers 2017 Psud
- [7] Jimmy ROUSSEL Optique géométrique [https ://femto-physique.fr/optique/](https://femto-physique.fr/optique/)
- [8] C. Leluc, Université de Genève , "Optique ondulatoire-la diffraction"

Annexe : Characteristics of the $f_0=100$ lens

